# Magnetosonic waves propagation in a magnetorotating quantum plasma

Yusra A. A. Hager [1,*] Mahmood A. H. Khaled [2] and Mohamed A. Shukri[2]
[1]*Department of Physics, Faculty of Education, Sana'a University, Sana'a, Yemen*
[2]*Department of Physics, Faculty of Science, Sana'a University, Sana'a, Yemen*

Employing the quantum magnetohydrodynamic (QMHD) model, the basic properties of magnetosonic waves were investigated in a magnetorotating quantum plasma. The contemplated system considered a combined effects of quantum tunneling and degeneracy forces, dissipation influence, spin magnetization, in addition to the Coriolis force. Fast and slow magnetosonic modes were obtained and examined in the linear regime. Their frequencies are significantly modified due to the rotating parameters (frequency and angle) in addition to quantum correction effects. The nonlinear Korteweg–de Vries–Burger equation was derived using the reductive perturbation approach in a small amplitude limit. The aspects of magnetosonic shock profiles were explored analytically by applying the Bernoulli equation approach and numerically using the Runge-Kutta method. The regarded plasma parameters due to the investigated effects were found to play major roles in specifying the nature of monotonic and oscillatory shock waves' structures and their features. Our results may be applicable in magnetorotating quantum plasma in astrophysical environments such as neutron stars and white dwarfs.

## I. INTRODUCTION

It is well known that the dynamics of charged particles in dense plasmas (which are characterized by very high number density and very low temperature) are quite different from those in ordinary plasmas (i.e., plasma with low number density and high temperature). In dense plasmas, electrons become degenerate and the thermal de Broglie's wavelength becomes large compared with the average interparticle distance. Accordingly, such dense plasma acts like a Fermi gas and the quantum effects play a significant role in the charged particle's dynamics [1–4]. In fact, interest in quantum plasmas as an important research field of plasma physics dates backs to the 1950s, focusing on quantum electron gas in a metal in the framework of quantum kinetic equations [5–7]. Nowadays, quantum plasma has become one of the most important branches of plasma physics that has attracted the interest of many researchers due to its main role in understanding various astrophysical and cosmological systems like planetary interiors, compact astrophysical objects (such as, particularly, in the interior of Jupiter, white dwarfs, magnetar, superdense neutron star, black holes) [8–12], in addition to its applications in many industries such as semiconductor devices, micromechanical systems [13], ultracold plasmas [14,15], intense laser-plasma interaction experiments, quantum x-ray, and free-electron lasers [16].

Recently, there has been an increasing interest in studying magnetohydrodynamic waves in quantum magnetized plasmas that is based on a quantum magnetohydrodynamic (QMHD) approach [17–30]. Marklund and Brodin [17,18] extended the QMHD approach, including spin-1/2 effect of degenerate electrons in strongly magnetized quantum plasmas. Later on, quantum tunneling and electron spin influences were studied by many authors to investigate arbitrary [19,26] and small magnetosonic solitons in two and multicomponent quantum plasmas [20,21,29] either in one- [24] or two-dimensional systems [22–24]. Moreover, both spin-up and spin-down states of degenerated electrons were explored in linear and nonlinear regimes [28–30].

On the other hand, the rotational impacts were investigated in various magnetized plasmas, including the Coriolis force effect. Most studies neglected quantum effects. However, quantum effects have an important role in many real situations in magnetized quantum plasmas. Sahu *et al.* [31] investigated linear and nonlinear ion acoustic waves in quantum plasma considering the Coriolis force effect in addition to the effects of Fermi pressure and the Bohm potential. Other authors studied heavy nucleus-acoustic shock waves [32,33] in a relativistic quantum magneto-plasma under Coriolis force impacts and studied the features of small [32] and large amplitude [33] getting waves. Recently, Hussain *et al.* [34] studied the magnetized quantum plasma system under the effects of Coriolis force, quantum corrections, and spin polarization by employing the QHD model.

From all the above works, we found the investigation of magnetosonic waves considering quantum effects beside Coriolis force and plasma rotation influences based on QMHD theory was lacking. Thus, the basic aim of the present work is to investigate the linear and nonlinear properties of magnetosonic modes in quantum plasma with the effects of Coriolis force, quantum tunneling, quantum statistics, and spin magnetization contributions. The paper is organized as follows. Section II is devoted to the formulation of the theoretical model using basic equations from the QMHD theory, considering quantum corrections, magnetization, and rotation

*Corresponding author: hager22013@gmail.com

impacts. Section III, includes linearized perturbation equations and the modified dispersion relation is obtained and discussed analytically and numerically. In Sec. IV, the nonlinear properties of the shock magnetosonic waves are investigated by deriving Korteweg–de Vries—Burgers (KdVB) equation. Further, analytical and numerical discussions are presented in Sec. IV. Finally, we summarize our results in the concluding Sec. V.

## II. THEORETICAL MODEL AND QMHD EQUATIONS

We consider a two-component quantum magnetoplasma system composed of degenerate electrons and nondegenerate massive, positive ions fluids, including Bohm potential and electron spin-1/2 effects. The plasma system is supposed to be immersed in a uniform external magnetic field along the $z$ axis, i.e., $\mathbf{B}_0 = B_0\hat{\boldsymbol{e}}_z$ where $B_0$ represents the magnetic field strength and $\hat{\boldsymbol{e}}_z$ is the unit vector along the $z$ direction. The quantum effects of ions are assumed negligible due to their larger mass. Further, we assume here that the plasma system is slowly rotating with a rotational frequency $\Omega$ around an axis lying in the $x$-$z$ plane due to the Coriolis force effect. The one-fluid QMHD model for our plasma system can be developed by starting with the usual hydrodynamic fluid equations for the plasma species separately as follows.

The ion momentum equation is described as

$$n_i m_i \frac{D\mathbf{u}_i}{Dt} = e n_i(\mathbf{E} + \mathbf{u}_i \times \mathbf{B}) + 2n_i m_i(\mathbf{u}_i \times \boldsymbol{\Omega}) - \mathbf{R}_{ei}, \quad (1)$$

and the ion continuity equation gives

$$\frac{\partial n_i}{\partial t} + \boldsymbol{\nabla} \cdot (n_i \mathbf{u}_i) = 0. \quad (2)$$

Since we consider low-frequency perturbations (in comparison with electron gyrofrequency). Thus, the momentum equation of degenerate electrons reads

$$n_e m_e \frac{D\mathbf{u}_e}{Dt} = -n_e e(\mathbf{E} + \mathbf{u}_e \times \mathbf{B}) - \nabla P_{\mathrm{Fe}} + \mathbf{F}_Q + \mathbf{R}_{ei}, \quad (3)$$

and the electron continuity equation gives

$$\frac{\partial n_e}{\partial t} + \boldsymbol{\nabla} \cdot (n_e \mathbf{u}_e) = 0, \quad (4)$$

where $\frac{D}{Dt} = \frac{\partial}{\partial t} + \mathbf{u}_i \cdot \boldsymbol{\nabla}$ is the convective derivation; $m_i$ is the ion mass, $e$ is the electron charge, $\mathbf{u}_i$ ($\mathbf{u}_e$) and $n_i$ ($n_e$) are the velocity and number density of ions (electrons), and $\mathbf{E}$ is the electrostatic field. Here, $\mathbf{R}_{ei} = nm_e\nu_{ei}(\mathbf{u}_i - \mathbf{u}_e) = en_0\eta\mathbf{J}_p$ [35] is the rate of the transfer of momentum from ions to electrons by collisions where $\mathbf{J}_p$ is the current density and $\eta = m_e\nu_{ei}/e^2 n_0$ is the plasma resistivity in which $\nu_{ei}$ denotes electron-ion collisional frequency, $m_e$ is the electron mass, and $n_0$ is the unperturbed number density of particles. With the quasineutrality condition $n_e \approx n_i = n$, the current density $\mathbf{J}_p$ is thus given by

$$\mathbf{J}_p = en_i\mathbf{u}_i - en_e\mathbf{u}_e \approx en(\mathbf{u}_i - \mathbf{u}_e). \quad (5)$$

The Fermi's pressure for degenerate electrons ($P_{\mathrm{Fe}}$) can be expressed as [36,37]

$$P_{\mathrm{Fe}} = \frac{2}{5}\varepsilon_{\mathrm{Fe}}n_0\left(\frac{n_e}{n_0}\right)^{5/3}, \quad (6)$$

where $\varepsilon_{\mathrm{Fe}} = (3\pi^2 n_0)^{2/3}\hbar^2/2m_e$ is the Fermi energy of a degenerate electron. The $\mathbf{F}_Q$ term shown in Eq. (3) would be [19]

$$\mathbf{F}_Q = \frac{\hbar^2 n_e}{2m_e}\boldsymbol{\nabla}\left(\frac{\nabla^2\sqrt{n_e}}{\sqrt{n_e}}\right) + n_e\mu_B \tanh\left(\frac{\mu_B B}{\varepsilon_{\mathrm{Fe}}}\right)\boldsymbol{\nabla}B. \quad (7)$$

The first term in the above equation represents the Bohm potential gradient force due to the quantum tunneling effect while the second one is the electron spin magnetization force, $\mu_B = e\hbar/2m_e$ denotes the Bohr's magneton and $B = |\mathbf{B}|$. The $\tanh(\mu_B B/\varepsilon_{\mathrm{Fe}})$ function in Eq. (7) represents the Langevin function due to the magnetization of an electron spin 1/2. In the most dense plasma systems, the condition $\mu_B B \ll \varepsilon_{\mathrm{Fe}}$ is satisfied, and thus we can use the approximation $\tanh(\mu_B B/\varepsilon_{\mathrm{Fe}}) \approx \mu_B B/\varepsilon_{Fe}$.

The relevant Maxwell equations are

$$\boldsymbol{\nabla}\times\mathbf{B} = \mu_0(\mathbf{J}_p + \mathbf{J}_m), \quad (8)$$

$$\boldsymbol{\nabla}\times\mathbf{E} = -\frac{\partial\mathbf{B}}{\partial t}, \quad (9)$$

$$\boldsymbol{\nabla}\cdot\mathbf{B} = 0, \quad (10)$$

where $\mu_0$ is the permeability of free space and $\mathbf{J}_m = \boldsymbol{\nabla}\times\mathbf{M}$ is the spin magnetization current density of electrons. $\mathbf{M}$ is the mean magnetization. For $\varepsilon_{\mathrm{Fe}} \gg \mu_B B$, the magnetization increases linearly with $B$, so it can be approximated as

$$\mathbf{M} = n_e\mu_B\tanh\left(\frac{\mu_B B}{\varepsilon_{Fe}}\right)\hat{\mathbf{b}} \approx n_e\left(\frac{\mu_B^2 B}{\varepsilon_{Fe}}\right)\hat{\mathbf{b}},$$

where $\hat{\mathbf{b}} = \mathbf{B}/B$ is the unit vector in the $\mathbf{B}$ direction. The displacement current was removed from Eq. (8) owing to its small effect in the conducting plasma medium in comparison to the total current density. Now, substituting $\mathbf{u}_e$ from Eq. (5) into Eq. (3) and neglecting the electron inertia because its mass is much smaller than the ion mass (i.e., $m_e/m_i \to 0$). Then, we obtain the generalized form of Ohm's law as

$$\mathbf{E} + \mathbf{u}_i\times\mathbf{B} = \frac{1}{en}(\mathbf{J}_p\times\mathbf{B} - \nabla P_{\mathrm{Fe}} + \mathbf{F}_Q + \mathbf{R}_{ei}). \quad (11)$$

Eliminating $\mathbf{E}$ between Eqs. (11) and (1), and substituting from Eq. (8) to eliminate $\mathbf{J}_p$, we obtain

$$nm_i\frac{D\mathbf{u}_i}{Dt} = \frac{1}{\mu_0}(\boldsymbol{\nabla}\times\mathbf{B})\times\mathbf{B} - (\boldsymbol{\nabla}\times\mathbf{M})\times\mathbf{B} - \nabla P_{\mathrm{Fe}}$$
$$+ \mathbf{F}_Q + 2nm_i(\mathbf{u}_i\times\boldsymbol{\Omega}), \quad (12)$$

Eliminating again $\mathbf{E}$ between Eqs. (9) and (11) and utilizing Eq. (8) to eliminate $\mathbf{J}_p$, then the magnetic induction equation can be obtained as

$$\frac{\partial\mathbf{B}}{\partial t} = \boldsymbol{\nabla}\times(\mathbf{u}_i\times\mathbf{B}) - \frac{1}{\mu_0}\boldsymbol{\nabla}\times(\eta\boldsymbol{\nabla}\times\mathbf{B}). \quad (13)$$

Here, we used the fact that the divergence of a curl always vanishes and neglects the Hall effect where the ion gyrofrequency is assumed to be much higher than the wave frequency. Now, we introduce the following dimensionless variables: $\tilde{\boldsymbol{r}} = \boldsymbol{r}\omega_{ci}/V_A$, $\mathbf{u} = \mathbf{u}_i/V_A$, $\tilde{\mathbf{B}} = \mathbf{B}/B_0$, $\tilde{t} = \omega_{ci}t$, $\tilde{n} = n/n_0$, $\tilde{\mathbf{M}} = \mu_0\mathbf{M}/B_0$, and $\tilde{\boldsymbol{\Omega}} = \boldsymbol{\Omega}/\omega_{ci}$ where $\omega_{ci} = eB_0/m_i$ is the ion gyrofrequency and $V_A = B_0/\sqrt{\mu_0 n_0 m_i}$ is Alfvén speed. The

magnetization normalized as $\tilde{\mathbf{M}} = \mu_0 \mathbf{M}/B_0$. Consequently, the normalized QMHD equations become

$$\frac{\partial \tilde{n}}{\partial \tilde{t}} + \nabla \cdot (\tilde{n}\mathbf{u}) = 0, \tag{14}$$

$$\tilde{n}\frac{D\mathbf{u}}{D\tilde{t}} = (\nabla \times \tilde{\mathbf{B}}) \times \tilde{\mathbf{B}} - \varepsilon_0^2 \beta (\nabla \times \tilde{n}\tilde{\mathbf{B}}) \times \tilde{\mathbf{B}} - \frac{1}{3}\beta \tilde{n}^{\frac{2}{3}} \nabla \tilde{n}$$

$$+ \frac{H^2}{2}\tilde{n}\nabla\left(\frac{\nabla^2\sqrt{\tilde{n}}}{\sqrt{\tilde{n}}}\right) + \varepsilon_0^2 \beta \tilde{n}\tilde{B}\nabla\tilde{B} + 2\tilde{n}(\mathbf{u}\times\tilde{\boldsymbol{\Omega}}), \tag{15}$$

$$\frac{\partial \tilde{\mathbf{B}}}{\partial \tilde{t}} = \nabla \times (\mathbf{u}\times\tilde{\mathbf{B}}) + \gamma\nabla^2\tilde{\mathbf{B}}, \tag{16}$$

where we use $\tilde{\mathbf{M}} = \varepsilon_0^2 \beta \tilde{n}B\hat{\mathbf{b}}$ in Eq. (15) and the vector identity $\nabla\times(\nabla\times\tilde{\mathbf{B}}) = \nabla(\nabla\cdot\tilde{\mathbf{B}}) - \nabla^2\tilde{\mathbf{B}}$ with $\nabla\cdot\tilde{\mathbf{B}} = 0$ in Eq. (16). The $\nabla\times(\mathbf{u}\times\tilde{\mathbf{B}})$ term in Eq. (16) represents the flow term, which dominates for larger plasma conductivity, while the $\gamma\nabla^2\tilde{\mathbf{B}}$ term is called the magnetic diffusion term, with $\gamma = \eta\omega_{ci}/\mu_0 V_A^2$ denoting the dimensionless plasma dissipative parameter (normalized magnetic diffusion coefficient). Here, $\varepsilon_0 = \mu_B B_0/\varepsilon_{\mathrm{Fe}}$ is the ratio of the Zeeman energy to the Fermi energy, $\beta = C_s^2/V_A^2$ is the plasma beta factor, $C_s = (2\varepsilon_{\mathrm{Fe}}/m_i)^{1/2}$ is the quantum ion sound speed, and $H = \hbar\omega_{ci}/\sqrt{m_e m_i}V_A^2$ is a dimensionless quantum diffraction parameter.

Assuming that the magnetosonic waves are propagated along the $x$-direction and the magnetic field and spin magnetization are supposed to be along the $z$ direction as $\tilde{\mathbf{B}} = \tilde{B}(\tilde{x},\tilde{t})\hat{\boldsymbol{e}}_z$ and $\tilde{\mathbf{M}} = \tilde{M}(\tilde{x},\tilde{t})\hat{\boldsymbol{e}}_z$, respectively; the plasma rotates slowly around an axis making the $\theta$ angle with the $z$ axis. Thus, in a one-dimensional Cartesian coordinate system, $\nabla = (\partial\tilde{x}, 0, 0)$ and $\tilde{\boldsymbol{\Omega}} = (\Omega_0\sin\theta, 0, \Omega_0\cos\theta)$. Then, one can reduce the normalized Eqs. (14) to (16) to

$$\frac{\partial \tilde{n}}{\partial \tilde{t}} + \frac{\partial}{\partial \tilde{x}}(u_x\tilde{n}) = 0, \tag{17}$$

$$\tilde{n}\left(\frac{\partial u_x}{\partial \tilde{t}} + u_x\frac{\partial u_x}{\partial \tilde{x}}\right) = \left(2\varepsilon_0^2\beta\tilde{n} - 1\right)\tilde{B}\frac{\partial\tilde{B}}{\partial\tilde{x}} + \varepsilon_0^2\beta\tilde{B}^2\frac{\partial\tilde{n}}{\partial\tilde{x}}$$

$$- \frac{\beta}{3}\tilde{n}^{2/3}\frac{\partial\tilde{n}}{\partial\tilde{x}} + \frac{H^2}{2}\tilde{n}\frac{\partial}{\partial\tilde{x}}\left(\frac{1}{\sqrt{\tilde{n}}}\frac{\partial^2\sqrt{\tilde{n}}}{\partial\tilde{x}^2}\right)$$

$$+ 2\Omega_0\tilde{n}u_y\cos\theta, \tag{18}$$

$$\frac{\partial u_y}{\partial \tilde{t}} + u_x\frac{\partial u_y}{\partial \tilde{x}} = 2\Omega_0(u_z\sin\theta - u_x\cos\theta), \tag{19}$$

$$\frac{\partial u_z}{\partial \tilde{t}} + u_x\frac{\partial u_z}{\partial \tilde{x}} = -2\Omega_0 u_y\sin\theta, \tag{20}$$

$$\frac{\partial \tilde{B}}{\partial \tilde{t}} + \frac{\partial}{\partial \tilde{x}}(u_x\tilde{B}) - \gamma^2\frac{\partial^2\tilde{B}}{\partial\tilde{x}^2} = 0. \tag{21}$$

### III. LINEAR ANALYSIS

To analyze the linear features of the magnetosonic waves, we deduce their linear dispersion relation. For this purpose, we assume first that all variable quantities (i.e., $n, u_x, u_y, u_z, B$) are separated into a two-term, namely, the equilibrium quantity ($f_0$) and perturbed quantity

($f_1$) such as $f = f_0 + f_1$, where $f = (n, u_x, u_y, u_z, B)$, $f_0 = (1, 0, 0, 0, 1)$ and $f_1$ corresponds to small perturbations i.e., $f_1 = (n_1, u_{x1}, u_{y1}, u_{z1}, B_1)$. Second, we consider all perturbed quantities are proportional to $\exp i(kx - \omega t)$, where $k$ is the wave number and $\omega$ represents the wave frequency. Linearizing Eqs. (17) to (21) using $\partial/\partial\tilde{t} = -i\omega$ and $\partial/\partial\tilde{x} = ik$, the following linearized equations are obtained:

$$\omega n_1 - ku_{x1} = 0, \tag{22}$$

$$\omega u_{x1} = \left(1 - 2\varepsilon_0^2\beta\right)kB_1 - k\varepsilon_0^2\beta n_1 + \frac{\beta}{3}kn_1$$

$$+ k^3\frac{H^2}{4}n_1 + 2i\Omega_0 u_{iy1}\cos\theta, \tag{23}$$

$$\omega u_{y1} - 2i\Omega_0 u_{z1}\sin\theta + 2i\Omega_0 u_{x1}\cos\theta = 0, \tag{24}$$

$$\omega u_{z1} + 2i\Omega_0 u_{y1}\sin\theta = 0, \tag{25}$$

$$(\omega + i\gamma k^2)B_1 - ku_{x1} = 0. \tag{26}$$

Solving the set of linear system of Eqs. (22) to (26), we obtain the following dispersion relation:

$$\omega(\omega^4 - a_1 k^2\omega^2 - a_2 k^2) + i\gamma k^2(\omega^4 - b_1 k^2\omega^2 - b_2 k^2) = 0, \tag{27}$$

in which the coefficients $a_1, a_2, b_1,$ and $b_2$ are defined as

$$a_1 = 1 - b_1 - 2\beta\varepsilon_0^2,$$
$$a_2 = b_2 + 4\Omega_0^2\sin^2\theta\left(2\beta\varepsilon_0^2 - 1\right),$$

and

$$b_1 = \frac{1}{4}k^2 H^2 - \frac{1}{3}\beta\left(3\varepsilon_0^2 - 1\right) + 4\frac{\Omega_0^2}{k^2},$$

$$b_2 = \frac{\Omega_0^2\sin^2\theta}{3}\left[4\beta\left(3\varepsilon_0^2 - 1\right) - 3H^2 k^2\right].$$

Equation (27) describes the magnetosonic wave propagating perpendicular to the ambient magnetic field. It is modified by the presence of rotating and dissipation effects as well as quantum effects. Ignoring the rotating effect (via $\Omega_0 = 0$), we get $a_2 = b_2 = 0$, and Eq. (27) turns into the same result given in Refs. [26] and [38]. It is noted that the imaginary part of Eq. (27) reflects the energy dissipation associated with plasma resistivity (via $\gamma$ parameter). In the case of perfect conductivity, $\gamma \approx 0$, then Eq. (27) reduces to

$$\omega^4 - a_1 k^2\omega^2 - a_2 k^2 = 0, \tag{28}$$

whose solution takes the following form:

$$\omega = \frac{k}{\sqrt{2}}(a_1 \pm \sqrt{a_1^2 + 4a_2/k^2})^{1/2}, \tag{29}$$

where the condition $(a_1^2 + 4a_2/k^2) \geqslant 0$ must be satisfied for real values of $\omega$. Clearly, Eq. (29) indicates that there are two magnetosonic waves that may exist in the current quantum plasma system, namely, fast magnetosonic waves ($\omega_f$) and slow magnetosonic waves ($\omega_s$). The wave with the plus sign in Eq. (29) is comparable to the fast magnetosonic wave, while that with the minus sign is comparable to the slow magnetosonic wave. To investigate the modified features of
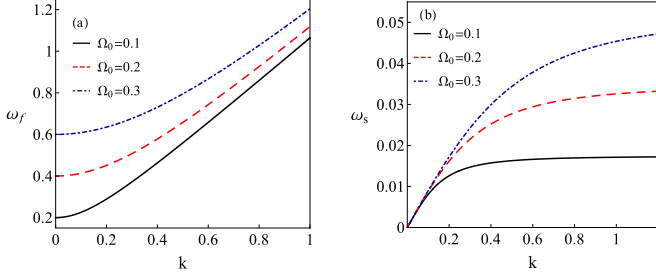
FIG. 1. Dispersion relation of (a) fast and (b) slow magnetosonic waves against the wave number $k$ for different values of $\Omega_0$ with $n_0 = 2 \times 10^{32}$ m$^{-3}$, $B_0 = 0.6 \times 10^6$ T, $\theta = 5°$, $H = 0.00018$, $\varepsilon_0 = 0.028$, and $\beta = 0.28$.

the fast and slow magnetosonic waves, we illustrate the dispersion characteristics in Figs. 1 and 2 for various plasma coefficients. Our investigation is based on suitable and real situations in magnetized quantum plasma systems found in dense astrophysical objects such as neutron stars and white dwarfs. Thus, the parameters used for $\beta$, $H$, and $\varepsilon_0$ are expressed numerically in terms of their exact relations as $\beta = 1.47 \times 10^{-43}(n_0^{5/3}/B_0^2)$, $H = 5.44 \times 10^{-31}(n_0/B_0)$, $\varepsilon_0 = 1.59 \times 10^{14}(B_0/n_0^{2/3})$. Such systems' suitable parameters are $n_0 = 10^{32} - 10^{35}$ m$^{-3}$ for the plasma densities and for magnetic field strength $B_0 = 10^5 - 10^{10}$ T.

Figure 1(a) shows how the fast magnetosonic wave frequency is modified due to the wave number $k$ and rotation speed $\Omega_0$. It is found that, due to an increase in rotation speed and wave number, the fast magnetosonic wave frequency $\omega_f$ increases. The rotation speed $\Omega_0$ has a significant effect for small $k$ and the influence becomes weaker as $k$ is increased. Figure 1(b) indicates that increasing the rotation speed $\Omega_0$ increases the frequency of the slow magnetosonic wave $\omega_s$. It is initially demonstrated by a nearly linearly increase for small $k$, and then when $k > 0.2$ it increases as $\Omega_0$ increases. Figure 2 clarifies the impact of the rotational angle $\theta$ on the magnetosonic wave frequency. It is clear from Fig. 2(a) that $\omega_f$ is slightly regressed as $\theta$ is increased; the effect is very weak for smaller $k$ values. Moreover, a deviation behavior is noted in Fig. 2(b) for the slow mode, as $\theta$ increases $\omega_s$ is getting larger. The figure shows a linear relation with $k$ which changes to be invariant as the wave number becomes higher.
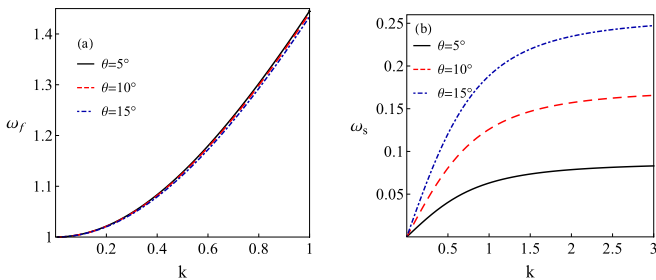


FIG. 2. Dispersion relation of (a) fast and (b) slow magnetosonic waves against the wave number $k$ for different values of $\theta$ with $n_0 = 2 \times 10^{32}$ m$^{-3}$, $B_0 = 0.6 \times 10^6$ T, $\Omega_0 = 0.5$, $H = 0.00018$, $\varepsilon_0 = 0.028$, and $\beta = 0.28$.

## IV. NONLINEAR ANALYSIS

### A. KdVB equation derivation

The dynamics of the nonlinear propagation of small amplitude magnetosonic shock waves can be examined by employing the reductive perturbation technique in the rescaled stretched space and time coordinates as

$$\xi = \epsilon^{1/2}(x - \lambda t), \quad \tau = \epsilon^{3/2}t, \tag{30}$$

where $\lambda$ is the wave phase velocity normalized by Alfvén speed $V_A$, $\epsilon$ is a small parameter measuring the nonlinearity strength. The dynamical-dependent variables are expanded in terms of $\epsilon$ such as

$$\begin{pmatrix} \tilde{n} \\ u_x \\ u_z \\ \tilde{B} \end{pmatrix} = \begin{pmatrix} 1 \\ 0 \\ 0 \\ 1 \end{pmatrix} + \epsilon \begin{pmatrix} n_1 \\ u_{x1} \\ u_{z1} \\ B_1 \end{pmatrix} + \epsilon^2 \begin{pmatrix} n_2 \\ u_{x2} \\ u_{z2} \\ B_2 \end{pmatrix} + \cdots, \tag{31}$$

while $u_y$ can be expanded as

$$u_y = \epsilon^{3/2}u_{y1} + \epsilon^{5/2}u_{y2} + \cdots, \tag{32}$$

along with the resistive term expansion $\gamma = \epsilon^{1/2}\gamma_0$ [39]. Inserting Eqs. (30) to (32) into Eqs. (17) to (21), we obtain a set of equations for each order in $\epsilon$. By solving the lowest-order equations, we obtain the following relations:

$$n_1 = B_1 = \frac{u_{x1}}{\lambda}, \tag{33}$$

$$u_{z1} = \lambda \cot^2 \theta B_1, \tag{34}$$

$$u_{y1} = \frac{\lambda^2 \cot^2 \theta}{2\Omega_0 \sin^2 \theta} \frac{\partial B_1}{\partial \xi}, \tag{35}$$

where the normalized phase velocity $\lambda$ is expressed by

$$\lambda = \sqrt{\frac{3 + \beta - 9\varepsilon_0^2\beta}{3(1 + \cot^2 \theta)}}. \tag{36}$$

Now, with the aid of Eqs. (33) to (35), the second-order ($\epsilon^2$) equations give

$$u_{z2} = u_{x2} \cot \theta - \frac{\lambda^3 \cot \theta}{4\Omega_0^2 \sin^2 \theta} \frac{\partial^2 B_1}{\partial \xi^2}. \tag{37}$$

In a similar manner, the higher order ($\epsilon^{5/2}$) gives the following equations:

$$\frac{\partial n_1}{\partial \tau} - \lambda \frac{\partial n_2}{\partial \xi} + \frac{\partial u_{x2}}{\partial \xi} + \frac{\partial(u_{x2}n_1)}{\partial \xi} = 0, \tag{38}$$

$$\frac{\partial u_{x1}}{\partial \tau} - \lambda \frac{\partial u_{x2}}{\partial \xi} + u_{x1} \frac{\partial u_{x1}}{\partial \xi} + \left(1 - 2\varepsilon_0^2\beta\right)\frac{\partial B_2}{\partial \xi}$$
$$- \lambda n_1 \frac{\partial u_{x1}}{\partial \xi} + (1 - 2\varepsilon_0^2\beta)B_1 \frac{\partial B_1}{\partial \xi} + \frac{\beta}{3}\left(1 - 3\varepsilon_0^2\right)\frac{\partial n_2}{\partial \xi}$$
$$- 2\varepsilon_0^2\beta \frac{\partial n_1 B_1}{\partial \xi} + \frac{2\beta}{9}n_1 \frac{\partial n_1}{\partial \xi} - \frac{H^2}{4}\frac{\partial^3 n_1}{\partial \xi^3}$$
$$- 2\Omega_0 u_{y2} \cos \theta - 2\Omega_0 u_{y1}n_1 \sin \theta = 0, \tag{39}$$

$$\frac{\partial u_{z1}}{\partial \tau} - \lambda \frac{\partial u_{z2}}{\partial \xi} + u_{x1} \frac{\partial u_{z1}}{\partial \xi} + 2\Omega_0 u_{y2} \sin \theta = 0, \tag{40}$$

$$\frac{\partial B_1}{\partial \tau} - \lambda \frac{\partial B_2}{\partial \xi} + \frac{\partial u_{x1} B_1}{\partial \xi} + \frac{\partial u_{x2}}{\partial \xi} - \gamma_0 \frac{\partial^2 B_1}{\partial \xi^2} = 0. \qquad (41)$$

Solving Eqs. (38) to (41) with the help of Eqs. (33) to (35), the following equation is obtained:

$$\frac{\partial B_1}{\partial \tau} + Q B_1 \frac{\partial B_1}{\partial \xi} + R \frac{\partial^3 B_1}{\partial \xi^3} - D \frac{\partial^2 B_1}{\partial \xi^2} = 0. \qquad (42)$$

Equation (42) is called the KdVB equation, in which the coefficients of nonlinearity $Q$, dispersion $R$, and dissipation $D$, respectively, are given by

$$Q = \frac{18\lambda^2(1 + \cot^2\theta)^2 + 9 - 54\varepsilon_0^2\beta + 2\beta}{18\lambda(1 + \cot^2\theta)}, \qquad (43)$$

$$R = \frac{1}{8\lambda(1 + \cot^2\theta)}\left(\frac{\lambda^4 \cot\theta}{\Omega_0^2 \sin^2\theta} - H^2\right), \qquad (44)$$

$$D = \frac{\gamma_0[3\lambda^2(1 + \cot^2\theta) + 3\varepsilon_0^2\beta - \beta]}{6\lambda^2(1 + \cot^2\theta)}. \qquad (45)$$

Clearly, all of the coefficients $Q$, $R$, and $D$ are modified by rotation angle, whereas the rotating speed (via $\Omega_0$) and quantum diffraction (via $H$ parameter) are found only to modify the dispersion coefficient $R$. The dissipation coefficient $D$ is altered due to quantum effects and plasma resistivity (via $\gamma_0$ parameter).

### B. Analytical solution of KdVB equation

To solve the KdVB Eq. (42) analytically, we define the transformed coordinate $\chi = -(\xi - U_0\tau)$ of the comoving frame with $U_0$ speed. Using this transformed into Eq. (42) and integrating over the variable $\chi$ with applying the boundary conditions $B_1 = dB_1/d\chi = d^2B_1/d\chi^2 \to 0$ as $\chi \to \pm\infty$, we find

$$R \frac{d^2 B_1}{d\chi^2} + D \frac{dB_1}{d\chi} + \frac{Q}{2} B_1^2 - U_0 B_1 = 0. \qquad (46)$$

If the plasma is perfectly conductive (i.e., $\gamma \to 0$), the dissipation term is ignored $D = 0$, and then Eq. (42) reduces to the KdV equation, and therefore Eq. (46) takes the form

$$R \frac{d^2 B_1}{d\chi^2} + \frac{Q}{2} B_1^2 - U_0 B_1 = 0, \qquad (47)$$

which has a soliton solution in the form

$$B_1 = B_m \text{sech}^2\left(\frac{\chi}{L}\right), \qquad (48)$$

where $B_m = 3U_0/Q$ and $L = \sqrt{4R/U_0}$ are the amplitude and width of the magnetosonic soliton, respectively. Figure 3 shows the behavior of the magnetosonic soliton profile of the KdV equation for different values of normalized rotation speed $\Omega_0$. It is obvious from this figure that increasing the parameter $\Omega_0$ leads to a decrease in the width of the magnetosonic soliton while its amplitude remains constant. The effect of the rotational angle $\theta$ on the magnetosonic soliton is exhibited in Fig. 4. It is seen that, as the rotational angle $\theta$ increases, the magnetosonic soliton profiles become wider with lower amplitude. We keep the physical parameters of plasma density $n_0$ and magnetic field strength $B_0$ unchanged; the same as that displayed in Figs. 1 and 2. Consequently,
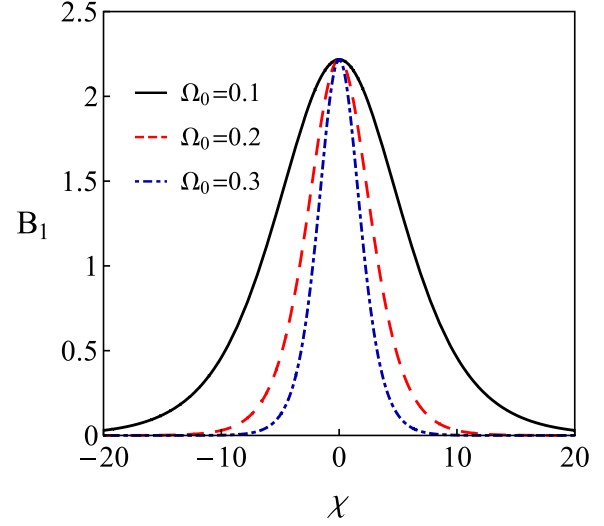


FIG. 3. The variation of magnetosonic soliton $B_1$ given by Eq. (48) against $\chi$ for different values of $\Omega_0$ with, $\gamma_0 = 0$, $U_0 = 0.1$, and $\theta = 5°$.

the quantum diffraction parameter $H$, Zeeman energy $\varepsilon_0$, and plasma beta factor $\beta$ are also the same as in Figs. 1 and 2.

Now, to obtain the KdVB equation solution, Bernoulli's equation method [40,41] will be used. With that method, the traveling wave solution of Eq. (46) is

$$B_1(\chi) = a_0 + a_1 G(\chi) + a_2 G^2(\chi), \qquad (49)$$

where $G(\chi) = \sigma/2\{1 + \tanh[(\sigma/2)\chi]\}$ is the solution of the following Bernoulli's equation:

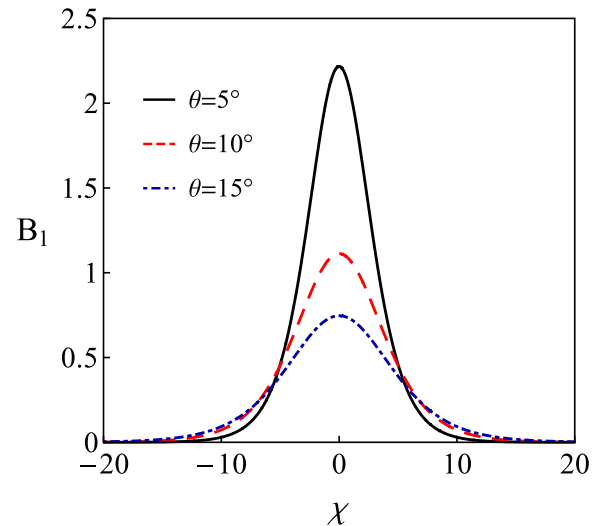$$\frac{\partial G(\chi)}{\partial \chi} = \sigma G(\chi) - G^2(\chi). \qquad (50)$$



FIG. 4. The variation of magnetosonic soliton $B_1$ given by Eq. (48) against $\chi$ for different values of $\theta$ with $\Omega_0 = 0.2$ and the same physical plasma parameters in Fig. 3.
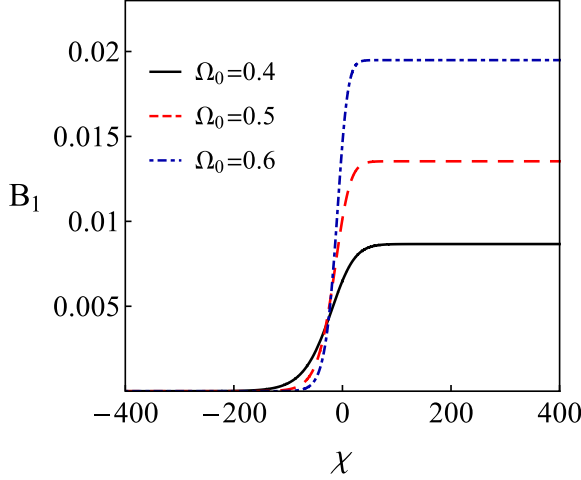
FIG. 5. The variation of magnetosonic shock wave profiles $B_1$ against $\chi$ for different values of $\Omega_0$ with $n_0 = 2 \times 10^{32}\,\mathrm{m}^{-3}$, $B_0 = 0.6 \times 10^6$ T, $\theta = 5°$, $\gamma_0 = 0.03$, $H = 0.00018$, $\varepsilon_0 = 0.028$, and $\beta = 0.28$.

The coefficients $a_0$, $a_1$, $a_2$, and $\sigma$ are constants to be determined later. Accordingly, the derivatives of $B_1$ with respect to $\chi$ are

$$\frac{\partial B_1}{\partial \chi} = (a_1 + 2a_2 G)(\sigma G - G^2), \qquad (51)$$

$$\frac{\partial^2 B_1}{\partial \chi^2} = [a_1(\sigma - 2G) + 2a_2(2\sigma G - 3G^2)](\sigma G - G^2). \quad (52)$$

Substituting Eqs. (49), (50), and (52) into Eq. (46) and collecting all terms with the same degree of $G$, the coefficients $a_0$, $a_1$, $a_2$, and $\sigma$ are obtained as

$$a_0 = \frac{2U_0}{Q}, \quad a_1 = 0, \quad a_2 = -\frac{12R}{Q}, \quad \sigma = -\frac{D}{5R},$$

where $U_0$ is calculated to be $U_0 = 6D^2/25R$. Accordingly, the localized solution of Eq. (42) is

$$B_1 = \frac{3D^2}{25QR}\left\{ \operatorname{sech}^2\left(\frac{D}{10R}\chi\right) + 2\left[1 + \tanh\left(\frac{D}{10R}\chi\right)\right]\right\}. \tag{53}$$

It is clear that the solution (53) is a combination of a solitary wave (sech$^2$) term and the Burger shock wave term (tanh). It is worthwhile to note that the amplitude of the Burger's shock term is larger than that of the solitary term. Hence, the Burger's shock wave is dominant. The formation of the nonlinear shock wave structures are shown graphically as given in Figs. 5–7. Figure 5 represents the variation of the magnetosonic shock wave profile $B_1(\chi)$ with rotation frequency $\Omega_0$. It is clear from this figure that the normalized shock wave amplitude is shifted to higher values with the increase of $\Omega_0$ while the normalized shock width becomes narrower. The effect of the rotating angle $\theta$ on the shock profile is depicted in Fig. 6. It is noticed that the larger rotating angle $\theta$ leads to wider shocks with lower amplitudes. The effect of plasma dissipating (via $\gamma_0$ dissipative parameter) on the profile of magnetosonic shocks is shown in Fig. 7. It is noticed that by
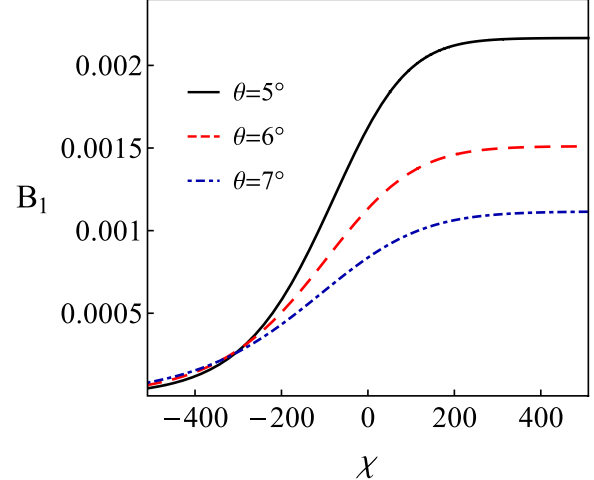
increasing the value of $\gamma_0$, the thickness (amplitude) of the shock is reduced (enhanced).

### C. Numerical solution

The discussed analytical solution of Eq. (42) introduced a monotonic shock structures. To investigate more possible structures and their features, we examine a numerical simulation solution of Eq. (42) with the help of MATHEMATICA software. For this purpose, we express Eq. (46) in terms of two separate first-order equations as

$$\frac{\partial B_1}{\partial \chi} = Z,$$

$$\frac{\partial Z}{\partial \chi} = \frac{U_0}{R}B_1 - \frac{Q}{2R}B_1^2 - \frac{D}{R}Z. \tag{54}$$

The above pair of equations has two fixed points, i.e., $(0, 0)$ and $(2U_0/Q, 0)$. Hence the dynamics of magnetosonic shock



FIG. 6. The variation of magnetosonic shock wave profiles $B_1$ against $\chi$ for different values of $\theta$ with $\Omega_0 = 0.2$, $\gamma_0 = 0.03$ and other parameters are the same as in Fig. 5.
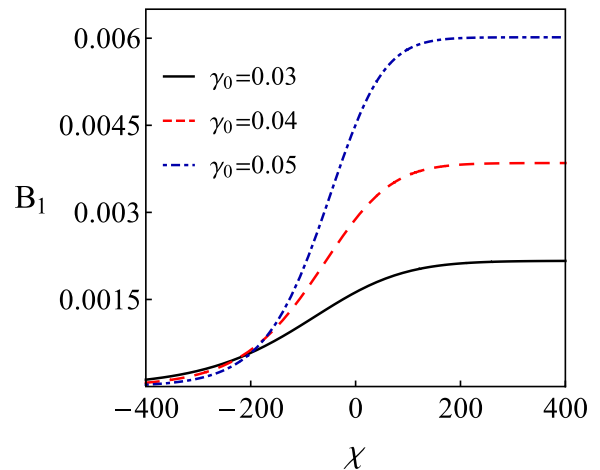


FIG. 7. The variation of magnetosonic shock wave profiles $B_1$ against $\chi$ for different values of $\gamma_0$ with $\Omega_0 = 0.2$, $\theta = 5°$ and other parameters are the same as in Fig. 5.
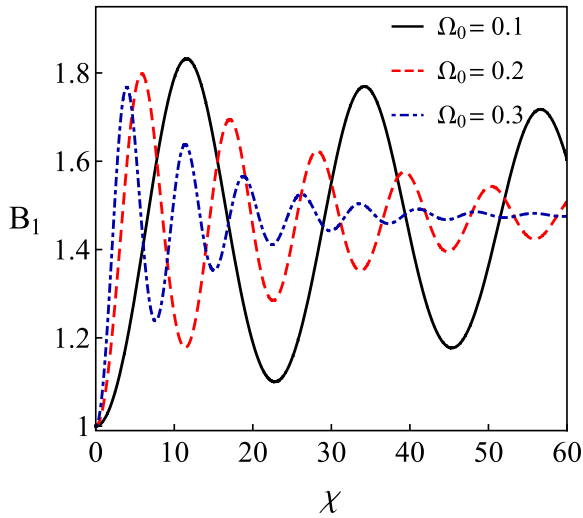
FIG. 8. Magnetosonic shock wave profile for different values of $\Omega_0$ where $\theta = 5°$, $\gamma_0 = 0.05$ and other parameters are the same as in Fig. 3.



FIG. 10. Magnetosonic shock wave profile for different values of $\gamma_0$ where $\Omega_0 = 0.3$, and other plasma parameters are the same as in Fig. 8.

waves can be investigated by solving the system of Eqs. (54) numerically using the fourth-order Runge Kutta method for different plasma configurations. Figure 8 depicts the influence of the rotation speed $\Omega_0$ on the shock structure's nature. It can be seen that as $\Omega_0$ increases the wave strength and width become smaller and tend to damp faster. Figure 9 illustrates how the oscillation shock profiles are affected by rotation angle $\theta$. It is clear that, as $\theta$ increases, the wave oscillates with less amplitude and tends to damp as $\chi$ progresses. The role of the dissipative parameter on the oscillation shock profiles is presented in Fig. 10. The wave profile oscillates more with large amplitude for weak resistivity parameter ($\gamma_0 = 0.05$), whereas the damping is found more prominent with less amplitude corresponding to larger $\gamma_0$ values (stronger dissipative coefficient). Figure 11 explicates the effect of the rotation

frequency for the case of the perfect conductivity medium ($\gamma_0 = 0.0001$). It is clear that the wave profile oscillation is periodic with the same amplitude whatever $\Omega_0$ value changes, whereas its width decreases as $\Omega_0$ increases. This reflects the same behavior of the magnetosonic soliton profile explored in Fig. 3 when the dissipation term is ignored.

## V. CONCLUSION

The current investigations are based on quantum magnetohydrodynamic theory to study the linear and nonlinear features of magnetosonic waves in magnetorotating degenerate quantum plasma, taking into account quantum corrections and rotational contributions for such plasma. It is found that the frequencies of both fast and slow magnetosonic waves
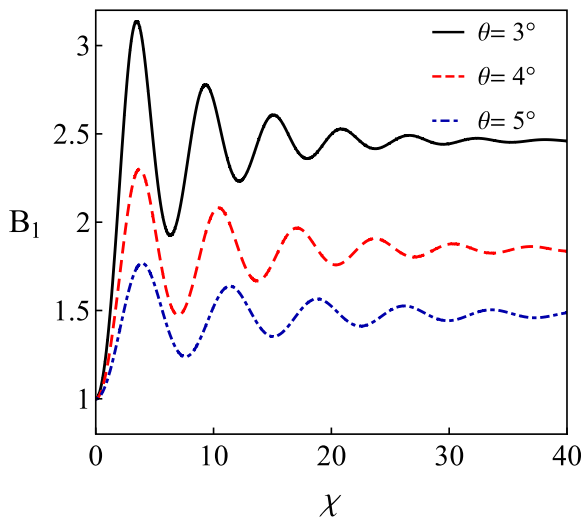


FIG. 9. Magnetosonic shock wave profile for different values of rotation angle $\theta$ where $\Omega_0 = 0.3$ and other parameters are the same as in Fig. 8.
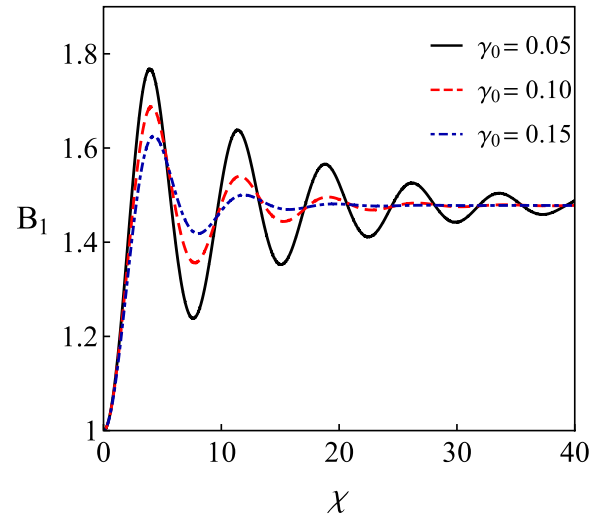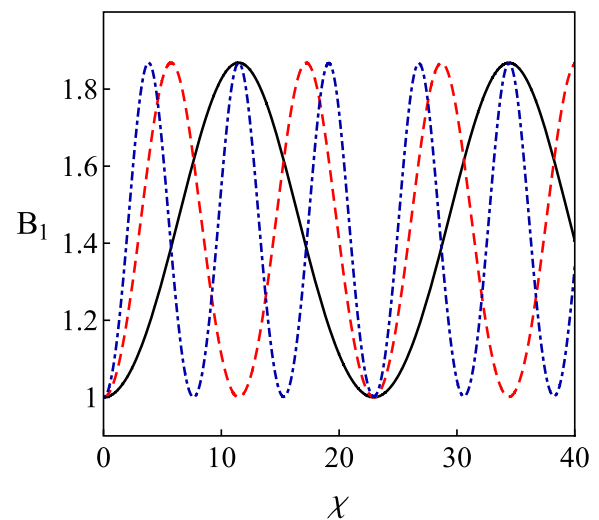


FIG. 11. Magnetosonic shock wave profile for different values of $\Omega_0$: $\Omega_0 = 0.1$ (solid curve), $\Omega_0 = 0.2$ (dashed curve), and $\Omega_0 = 0.3$ (dot dashed curve) with $\gamma_0 = 0.0001$, and $\theta = 5°$, other parameters are the same as in Fig. 8.

are significantly enhanced with the variation of rotation frequency and rotation angle. In the nonlinear regime, the KdVB equation was obtained employing the reductive perturbation technique. Bernoulli's equation method was presented to determine the characteristic of the shock wave solution nature. We noticed that the structure of shock waves is monotonic and its properties such as height and thickness depend on the quantum parameters, expressed in terms of density concentration and magnetic field, dissipation, in addition to rotation frequency and angle. Furthermore, a numerical analysis is performed to investigate the KdVB equation solution structures using the Runge-Kutta method by variation of our investigated plasma coefficients. We also explored their effects. It is found that numerical solutions conduce oscillatory shock wave profiles, higher values of dissipative parameter, and rotation coefficients resulting in damped oscillation waves with smaller amplitude. Such significant modifications of the shock-like structures in our rotating quantum plasma are relevant for strongly magnetized quantum plasma systems and useful for a better understanding of wave propagation in astrophysical environments, such as the magnetars, pulsars, magnetic white dwarfs, and neutron stars.

[1] P. K. Shukla and S. Ali, Phys. Plasmas **12**, 114502 (2005).

[2] S. Ali and P. K. Shukla, Phys. Plasmas **13**, 022313 (2006).

[3] P. K. Shukla and S. Ali, Phys. Plasmas **13**, 082101 (2006).

[4] S. Mahmood, Phys. Plasmas **15**, 014502 (2008).

[5] D. Bohm and D. Pines, Phys. Rev. **92**, 609 (1953).

[6] D. Pines, Phys. Rev. **92**, 626 (1953).

[7] K. Sawada, Phys. Rev. **106**, 372 (1957).

[8] A. K. Harding and D. Lai, Rep. Prog. Phys. **69**, 2631 (2006).

[9] E. García-Berro, S. Torres, L. G. Althaus, I. Renedo, P. Lorén-Aguilar, A. H. Córsico, R. D. Rohrmann, M. Salaris, and J. Isern, Nature (London) **465**, 194 (2010).

[10] S. L. Shapiro and S. A. Teukolsky, *Black Holes, White Dwarfs, and Neutron Stars: The Physics of Compact Objects* (Wiley VCH, Weinheim, Germany, 2004).

[11] S. Chandrasekhar, Astrophys. J. **74**, 81 (1931).

[12] S. Chandrasekhar, Philos. Mag. **11**, 592 (1931).

[13] A. Jungel, *Transport Equations for Semiconductor Devices* (Springer, Berlin, 2009).

[14] W. Li, P. J. Tanner, and T. F. Gallagher, Phys. Rev. Lett. **94**, 173001 (2005).

[15] R. S. Fletcher, X. L. Zhang, and S. L. Rolston, Phys. Rev. Lett. **96**, 105003 (2006).

[16] P. K. Shukla and B. Eliasson, Phys. Rev. Lett. **99**, 096401 (2007).

[17] M. Marklund and G. Brodin, Phys. Rev. Lett. **98**, 025001 (2007).

[18] G. Brodin and M. Marklund, New J. Phys. **9**, 277 (2007).

[19] M. Marklund, B. Eliasson, and P. K. Shukla, Phys. Rev. E **76**, 067401 (2007).

[20] W. Masood and A. Mushtaq, Phys. Lett. A **372**, 4283 (2008).

[21] A. P. Misra and N. K. Ghosh, Phys. Lett. A **372**, 6412 (2008).

[22] A. Mushtaq and A. Qamar, Phys. Plasmas **16**, 022301 (2009).

[23] W. Masood, Phys. Plasmas **16**, 042314 (2009).

[24] A. Mushtaq and S. V. Vladimirov, Phys. Plasmas **17**, 102310 (2010).

[25] F. Haas, *Quantum Plasma, A Hydrodynamic Approach* (Springer, New York, 2011).

[26] A. Mushtaq and S. V. Vladimirov, Eur. Phys. J. D **64**, 419 (2011).

[27] F. A. Asenjo, Phys. Lett. A **376**, 2496 (2012).

[28] P. A. Andreev, Phys. Rev. E **91**, 033111 (2015).

[29] R. Ahmad, N. Gul, M. Adnan, and F. Y. Khattak, Phys. Plasmas **23**, 112112 (2016).

[30] Z. Rahim, M. Adnan, and A. Qamar, Phys. Rev. E **100**, 053206 (2019).

[31] B. Sahu, A. Sinha, and R. Roychoudhury, Phys. Plasmas **26**, 072119 (2019).

[32] K. Singh, P. Sethi, and N. S. Sainic, Phys. Plasmas **26**, 092104 (2019).

[33] N. S. Saini, M. Kaur, and K. Singh, Waves Random Complex Media **32**, 743 (2022).

[34] S. Hussain, A. Abdikian, and H. Hasnain, Contrib. Plasma Phys. **61**, e202000189 (2021).

[35] J. P. Goedbloed and S. Poedts, *Principles of Magnetohydrodynamics* (Cambridge University Press, Cambridge, England, 2004).

[36] C. Kittel, *Introduction to Solid State Physics*, 8th ed. (John Wiley & Sons, New York, 2005).

[37] R. K. Pathria, *Statistical Mechanics* (Butterworth-Heinemann, Oxford, 1996).

[38] S. Li and J. Han, Phys. Plasmas **21**, 032105 (2014).

[39] M. Bartuccelli, P. Carbonaro, and V. Muto, Lett. Nuovo Cimento **42**, 279 (1985).

[40] M. Mirzazadeh, M. Eslami, E. Zerrad, M. F. Mahmood, A. Biswas, and M. Belic, Nonlinear Dyn. **81**, 1933 (2015).

[41] M. G. Hafez, M. R. Talukder, and M. Hossain Ali, Phys. Plasmas **23**, 012902 (2016).